Analysis of the magnetic properties of strongly anisotropic magnetics: terbium–yttrium iron garnets

A. S. Lagutin and R. F. Druzhinina

"Kurchatov Institute" Russian Scientific Center

(Submitted 14 April 1992)
Zh. Eksp. Teor. Fiz. **102**, 1860–1871 (December 1992)

A microscopic model, constructed in the anisotropic molecular field approximation, is proposed for describing the magnetic properties of rare-earth iron garnets with high crystallographic anisotropy in fields up to 500 kOe. An algorithm for calculating the magnetic properties, taking into account the changes in the rare-earth-ion spectrum, is presented. The theoretical results agree well, both qualitatively and quantitatively, with the experimental data.

INTRODUCTION

For the last two decades rare-earth iron garnets (REIG) have been widely investigated both experimentally and theoretically. On the one hand, these objects are of interest because of their extensive promising technical applications, which stem from their enormously diverse (composition-dependent) magnetic properties[1–4] and comparatively high magnetic ordering temperature ($T_c \approx 560$ K). On the other hand, in order to construct a theoretical description of REIG the conventional methods must sometimes be modified significantly because there are no appropriate small parameters. In particular, the phenomenological method of expanding the thermodynamic potential in a series in the order parameter,[5] a method widely and successfully employed for calculating the magnetic characteristics of weakly anisotropic crystals, is not always effective for REIG. At the same time, first-prinicples calculations of the macroscopic properties of these compounds have not yet been developed, because the constituent rare-earth ions are complicated multiparticle objects.

The aim of this work is to demonstrate for the example of the REIG system $Tb_xY_{3-x}Fe_5O_{12}$ (TYIG) a method of calculating the static magnetic properties of iron garnets. The method presented in this paper is a quantum-phenomenological method, as defined in Ref. 6. It is based on the very realistic assumption that the states of the $4f$ electrons of rare-earth (RE) ions in REIG, which mainly determine the magnetic characteristics of these materials, are well localized and closely associated with the electron states in free atoms (ions). The effect of the crystalline environment of the rare-earth ions and of an external magnetic field is taken into account on the basis of the stationary perturbation theory with the help of a model Hamiltonian $\hat{V}$,[7–9] which is constructed using the symmetry properties of the magnetic system of the crystal and includes the usual terms—the crystal-field operator, the exchange interaction operator, and an operator describing the Zeeman splitting of the levels of the rare-earth ion:

$$\hat{V} = \hat{H}_{CF} + \hat{H}_{EXC} + \hat{H}_{ZS}, \quad \hat{H} = \hat{H}_0 + \hat{V}, \tag{1}$$

where $\hat{H}_0$ is the Hamiltonian of the free ion. It is important to note that in the method described the requirement that each term of the operator $\hat{V}$ be small compared with $\hat{H}_0$, irrespective of the ratios of the components of $\hat{V}$, is the only restriction. The parameters of the Hamiltonian $\hat{V}$ (this concerns only the operator $\hat{H}_{CF}$), however, will be determined by fitting the theoretical results to the experimental results—this is what makes the approach "phenomenological."

1. THE HAMILTONIAN AND ITS PARAMETERS

It is known[10–12] that the cubic unit cell of REIG consists of eight $R_3Fe_5O_{12}$ molecules, where R is a rare-earth atom or yttrium, and includes 16 Fe^{3+} ions at positions with an octahedral oxygen environment (a positions), 24 Fe^{3+} ions in positions with a tetrahedral environment of oxygen anions (d positions), and six inequivalent c positions with dodecahedral oxygen environment, in each of which there are four rare-earth ions. In what follows it is useful to introduce several coordinate systems: the principal system (x, y, z), whose axes are directed along the edges of the cubic cell of the crystal, and six local systems (x_l, y_l, z_l; $l = 1...6$), associated with the c positions. The matrices A_i of the transformations from the principal coordinate system to the local systems are as follows

$$A_{1,2} = \begin{pmatrix} 2^{-1/2} & \pm 2^{-1/2} & 0 \\ \mp 2^{-1/2} & 2^{-1/2} & 0 \\ 0 & 0 & 1 \end{pmatrix}, \quad A_{3,4} = \begin{pmatrix} 0 & 2^{-1/2} & \pm 2^{-1/2} \\ 0 & \mp 2^{-1/2} & 2^{-1/2} \\ 1 & 0 & 0 \end{pmatrix},$$

$$A_{5,6} = \begin{pmatrix} 2^{-1/2} & 0 & \pm 2^{-1/2} \\ \mp 2^{-1/2} & 0 & 2^{-1/2} \\ 0 & 1 & 0 \end{pmatrix}. \tag{2}$$

Here the upper sign corresponds to the first index and the lower sign corresponds to the second index. In other words, the coordinate systems are rotated by angles of $\pm \pi/4$ as follows: 1 and 2 around the z axis, 3 and 4 around the x axis, and 5 and 6 around the y axis.

Crystal field. We employ the operator H_{CF} in the standard form for REIG,[6,13] taking into account the symmetry of the environment of the rare-earth ion, i.e., (in local coordinates),

$$H_{CF} = \alpha B_2^0 O_2^0 + \alpha B_2^2 O_2^2 + \beta B_4^0 O_4^0 + \beta B_4^2 O_4^2 + \beta B_4^4 O_4^4 + \gamma B_6^0 O_6^0 + \gamma B_6^2 O_6^2 + \gamma B_6^4 O_6^4 + \gamma B_6^6 O_6^6, \tag{3}$$

where α, β, and γ are the Stevens parameters and O_k^n are equivalent operators.[13] For example, $O_2^0 = 3\hat{J}_z^2 - J(J-1)$, $O_2^2 = \frac{1}{2}(\hat{J}_+^2 + \hat{J}_-^2)$. Here $\hat{J}_z$, $\hat{J}_+$, and $\hat{J}_-$ are, respectively, the operators of the z component and the circular projections of the total angular momentum J of the rare-earth ion. The local coordinate systems are convenient because the set of parameters B_k^q (see Table I) will be

 0038-5646/92/121001-07$05.00

TABLE I. Values of the parameters H_{CF} at $T = 4.2$ K (in units of 10^4 J/m^3).

x	B_2^0	B_2^2	B_4^0	B_4^2	B_4^4	B_6^0	B_6^2	B_6^4	B_6^6
0,41	84	184	−24	900	80	4	2	−2	−186
0,26	84	188	−24	900	80	4	2	−2	−186
0,1	88	190	−00	900	80	4	2	−2	−186

the same for all six c positions. We emphasize that we consider (3) not as the Hamiltonian of the rare-earth ion in the field of point charges but rather as some effective operator which takes into account the partial screening of this field by the external electrons of the rare-earth ion as well as covalence and other effects (see below). In this case the parameters B_k^q consists of a set of coefficients giving the best agreement between the calculations and the experimental data. This set is found by adjusting the initial values of B_k^q in the calculation of the anisotropy constants ot TYIG (K_1 and K_2) at $T = 4.2$ K with a low content of rare-earth ions and then comparing with the experimental data. The initial parameters in turn were determined by extrapolating to low temperatures and low terbium concentrations from the theoretical dependences $B_k^q(x, T)$ for $T > 40$ K and significant terbium content.[14]

Exchange and Zeeman interactions. The antiferromagnetic exchange interaction between the a and d iron sublattices is very strong [≈ 100 T (Refs. 15–17)]. For this reason, even in fields ≈ 10 T the iron magnetic subsystem of the REIG crystal can be regarded as a ferromagnetic matrix with magnetic moment equal to the difference of the magnetic moments of the d and a sublattices ($5\mu_B$ per formula unit). Since the exchange interaction between the rare-earth and Fe ions is significantly weaker [≈ 10 T (Ref. 15)], its effect on the magnitude of the iron moments can be neglected. Therefore, we consider the terbium ion to be paramagnetic in the exchange field of the iron subsystem and the external magnetic field. This is essentially the molecular-field approximation, and the exchange and Zeeman interaction Hamiltonian can be put into the following form with the help of the relation $\hat{S} = (g_J - 1)\hat{J}$, which is valid within a multiplet of the rare-earth ion:[6]

$$\hat{H}_Z = \mu_B g_J \hat{J} \mathbf{H}_{\text{eff}} + 2\mu_B \Sigma G_n^m O_n^m(\hat{L})\,\hat{S}\,\mathbf{H}_{\text{mol}}, \tag{4}$$

where $\hat{L}$, $\hat{S}$, and $\hat{J}$ are the operators of the orbital, spin, and total angular momenta of the rare-earth ion; G_n^m are the anisotropic-exchange parameters;[18,20] g_j is the g-factor for Tb^{3+}, and

$$\mathbf{H}_{\text{eff}} = \mathbf{H} + 2g_J^{-1}(g_J - 1)\mathbf{H}_{\text{mol}}, \tag{5}$$

$$\mathbf{H}_{\text{mol}} = (I_{1l}z_1^{(l)} + I_{2l}z_2^{(l)})(g_J - 1)\mathbf{S}_{\text{Fe}}/g_J\mu_B. \tag{6}$$

Here $g_J = 3/2$, $z_k^{(l)}$ is the number of nearest Fe neighbors for the rare-earth ion in the l th site, and I_{1l} and I_{2l} are the exchange interaction integrals between the l th terbium ion and one of the iron sublattices. The Hamiltonian $\mathbf{H}_{\text{eff}}$ is essentially the effective isotropic magnetic field acting on a rare-earth ion. On the basis of the value $\mu_0 H_{\text{exc}} = 28$ T, determined in Ref. 21 from measurements of the critical fields limiting the canted phases in TYIG, we obtain $I_{1l}z_1^{(l)} + I_{2l}z_2^{(l)} = -2.78 \cdot 10^{-22}$ J. Note that because the orbital angular momentum of the rare-earth ion is not "frozen," there is an anisotropic exchange interaction in REIG, which it would be wrong to ignore. We shall show that an alternative to using the Hamiltonian (4) could be to treat only the isotropic component of the exchange under the assumption that the spatial position of the vector $\boldsymbol{\sigma} = \mathbf{M}/Ng\mu_B$ ($\mathbf{M} = \mathbf{M}_d - \mathbf{M}_a$) is determined self-consistently by minimizing the free energy taking into account the splitting of the levels of the rare-earth ion in the crystal and effective fields. Then instead of a single equation for the mean field, we obtain three equations, one for each component of $\boldsymbol{\sigma}$. This approximation is called the anisotropic molecular field approximation,[8] and it is a parametrization of the anisotropic part of the exchange interaction in the form of a Hamiltonian similar to that of the electrostatic model. In this approach it is not necessary to include the additional anisotropic exchange parameters G_n^m in the calculations along with B_k^q.

Finally, taking into account also the Zeeman interaction for the iron subsystem, we obtain the final form of the perturbation operator per formula unit of TYIG:[22]

$$\hat{V} = -\frac{1}{2}\sum_{l=1}^{6}\left\{\sum_{k,q} B_k^q \delta_q O_k^q - g\mu_B(\mathbf{B}_{\text{mol}}^l + \mathbf{B}^l)\hat{J}\right\} - 2\mu_B \mathbf{B} S\boldsymbol{\sigma}, \tag{7}$$

where $B_{\text{mol}}^{(l)}$ is the molecular field in the l th and terbium sublattice, $\mathbf{B}$ and $\mathbf{B}^l$ are the external induction in the principal and local coordinate systems, δ_k are the Stevens parameters ($\delta_{1,2} = \alpha$; $\delta_{3,4,5} = \beta$; $\delta_{6,7,8,9} = \gamma$), $\hat{J}$ is the total angular momentum operator of the rare-earth ion, and S is the spin of the Fe^{3+} ion. The rare-earth sublattices are labeled in conformity with the transformations (2).

2. ALGORITHM OF THE NUMERICAL EXPERIMENT

The self-consistent problem is solved in several steps. In the first step the matrix of the operator $\hat{V}$ is diagonalized in the basis functions Ψ (SLGM) of the free terbium ion. The degree of degeneracy of the ground state multiplet of this ion $^7F_6$ is $N = 13$, which determines the order of the matrix $\langle\Psi|\hat{V}|\Psi\rangle$. The matrix elements are complex numbers, and for this reason the method of diagonalization of a real matrix of order $2N$ is used to find the eigenvectors $|il\rangle$ and the corresponding eigenvalues ε_{il} of the operator $\hat{V}$ (Ref. 23). The desired wave functions and eigenvalues have the following form:

$$|il\rangle = \sum_{M=-J}^{J} C_{JM}^{il}\Psi(SLJM), \qquad \varepsilon_{il} = \sum_{MM'} c_{LM}^{*il}\, c_{LM'}^{il}\langle\Psi|\hat{V}|\Psi\rangle, \tag{8}$$

where l is the number of the sublattice, $i = 1, 2, 3, \ldots, 2J + 1$; and the asterisk indicates complex conjugation. It is obvious that C_{LM} and ε_{il} depend implicitly on the parameters σ_x, σ_y,

and σ_z, whose values are not known (yet!). The following secular equation is solved for some initial values of these parameters satisfying the relation $\sigma_x^2+\sigma_y^2+\sigma_z^2=1$:

$$\mathrm{Det}\{\langle SLJM|V|SLJM'\rangle-\varepsilon_{il}\delta_{MM'}\}=0. \quad (9)$$

The second step is to find σ_k ($k=x,y,z$) in the process of minimizing the free energy

$$F(x,T)=-\frac{x}{6}T\sum_{l=1}^{6}\ln\sum_{i=1}^{13}\exp\left(\frac{-\varepsilon_{il}}{kT}\right)-2\mu_B S(\mathbf{H}\boldsymbol{\sigma}). \quad (10)$$

where x is the concentration of terbium ions, T is the temperature, and k is the Boltzmann constant. The minimum of the function $F(x, T)$ is sought in a very straightforward manner: The valleys of the surface $F(\sigma_x, \sigma_y, \sigma_z)$ are followed directly by trying different values of the vector $\boldsymbol{\sigma}$; in computer calculations this is much simpler than using the Sylvester criterion, which requires continuously the second derivatives of $F(x, T)$, the computational error in the calculation of which is very large.[24,25]

The method adopted in the present work to search for the extremal values of $F(x, T)$ had some peculiarities. We sometimes encountered a situation in which the natural error of the computer calculations was comparable to the energy change accompanying variation of σ, as happens in the case of a potential well with very gently sloping walls. Sometimes several closely spaced local minima separated by potential barriers were observed. The "deepest" minimum was determined, and the search was continued over the entire physically reasonable range of $\boldsymbol{\sigma}$. Since the function $F(\boldsymbol{\sigma})$ is continuous, the next solution could be found comparatively easily from the last point found. Analysis of the local environment and the symmetry group of the crystal also made it possible to narrow the range of admissible orientations of the vector σ. In particular, when the external field lay in the (110) plane, due to the existence of the two relations $\sigma_x^2+\sigma_y^2+\sigma_z^2=1$ and $\sigma_x=\sigma_y$ symmetry considerations reduce the number of unknown parameters to one.

The third step of the calculations (actually the second step) was fitting the initial parameters B_k^q, necessary for calculating the orientation of $\boldsymbol{\sigma}$, by comparing the theoretical and experimental dependence of the first and second anisotropy constant, K_1 and K_2, respectively, in the absence of a magnetic field. For TYIG with a low concentration of rare-earth ions at low temperatures the admissibility of using an expansion of the free energy F in the direction cosines (α_i) of the vector σ (Ref. 5) in the form

$$F=K_1(\alpha_1^2\alpha_2^2+\alpha_1^2\alpha_3^2+\alpha_2^2\alpha_3^2)+K_2(\alpha_1^2\alpha_2^2\alpha_3^2), \quad (11)$$

which is normally insufficient for describing the properties of REIG under these conditions, was proved by the good agreement between the computed and experimental magnetization curves as well as between the theoretical and experimental temperature dependences of the anisotropy constants.[14] The expansion (11) was very effective for TYIG with $x=0.4$, in our opinion, for two reasons: 1) the specific concentration dependence $K_1(x)$ with a maximum near $x=0.5$ (Ref. 26) at low temperatures and 2) the low content of rare-earth ions. According to Ref. 5, the values of K_1 and K_2 are as follows:

$$K_1=4(F_2-F_4),\quad K_2=27(F_3-F_4)-36(F_2-F_4), \quad (12)$$

where F_2, F_3, and F_4 are the free energy of TYIG in the absence of a magnetic field with the iron moment oriented along the two-, three-, and four-fold crystal axes, respectively.

Finally, the last step in the calculations is to calculate the magnetization of each rare-earth sublattice in local coordinates:

$$\mathbf{M}_l^0(x)=\frac{x\sum_{i=1}^{13}\sum_{MM'}C_{iM}^{*}C_{iM'}\langle JM|\hat{\mathbf{J}}|JM'\rangle\exp(-\varepsilon_{il}/kT)}{3\sum_{i=1}^{13}\exp(-\varepsilon_{il}/kT)}. \quad (13)$$

Next the moments of the Tb^{3+} ion are transformed into the general coordinate system $\mathbf{M}_l=A_l^{-1}\mathbf{M}_l^0(x)$ and the total magnetic moment of the crystal is found:

$$\mathbf{M}(x)=5\mu_B\boldsymbol{\sigma}+\frac{1}{2}\sum_{l=1}^{6}\mathbf{M}_l(x). \quad (14)$$

Thus, the numerical modeling gives the spectra of rare-earth ions in each of six nonequivalent positions in the crystal lattice and the arrangement and magnitude of the rare-earth and Fe moments at any temperature and in any external magnetic field.

3. RESULTS AND DISCUSSION

The computed magnetization curves for single crystals of the system $Tb_xY_{3-x}Fe_5O_{12}$ ($x=0.1$, 0.26, and 0.41) at $T=4.2$ K and for three orientations of the external magnetic field relative to the crystallographic axes of the crystal are displayed in Figs. 1–4. The figures also show, for comparison, the experimental results obtained in Ref. 21, which in fields up to 15 T are virtually identical to the data obtained previously in Ref. 27. We note that the agreement between theory and experiment is entirely satisfactory in all cases. The computed curves describe very well the qualitative picture of the evolution of the magnetization with increasing field. The quantitative disagreement sometimes arising between theory and experiment can be explained by two fac-

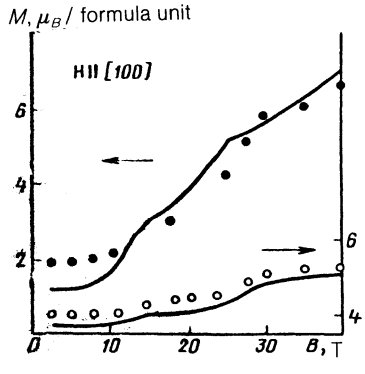

FIG. 1. Computed (dots) and experimental (solid lines) field dependence of the magnetic moment of a $Tb_xY_{3-x}Fe_5O_{12}$ single crystal at $T=4.2$ K in a magnetic field $B\parallel[100]$: $x=0.41$ (dark circles) and 0.1 (light-colored circles).

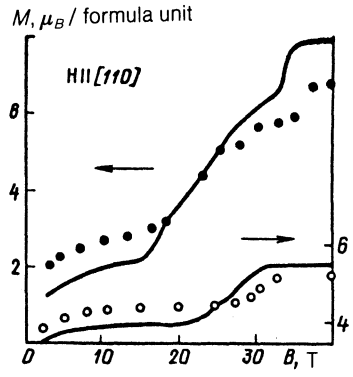

FIG. 2. Computed (dots) and experimental (solid lines) field dependences of the magnetic moment of a $Tb_xY_{3-x}Fe_5O_{12}$ single crystal at $T = 4.2$ K in a magnetic field $B \| [100]$: $x = 0.41$ (dark circles) and 0.1 (light-colored circles).

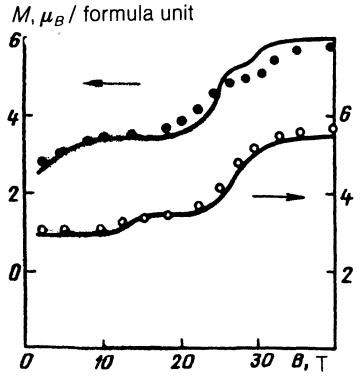

FIG. 4. Computed (dots) and experimental (solid lines) field dependences of the magnetic moment of a $Tb_{0.26}Y_{2.74}Fe_5O_{12}$ single crystal at $T = 4.2$ K in a magnetic field $B \| [110]$ (dark circles) and $B \| [100]$ (light circles).

tors. First, the measurements in Ref. 21 were conducted in pulsed magnetic fields, and it is known that under the specific conditions of the experiment the process of magnetization of REIG is nearly adiabatic, while the calculations were performed for isothermal magnetization. Second, we neglected the magnetostriction, due to which the lattice parameters change with the external field, and therefore both crystal-field parameters and, generally speaking, the exchange parameters. It is entirely possible to take into account the magnetoelastic interaction for REIG on the basis of the microscopic model developed in the present work, but this requires a much more complicated Hamiltonian because the local symmetry of the c positions is low. For this reason, the first version of the model presented in this paper was obtained neglecting striction. However, it became obvious that striction must be taken into account, and this was done in the further investigations.

The process of rearrangement of the magnetic structure of TYIG of different composition with increasing field, oriented along the two-, three-, and four-fold axes, is illustrated in Figs. 5–7. It is obvious that, in contrast to the $Ho_xY_{3-x}Fe_5O_{12}$,[28] in which the magnetization of the rare-earth subsystem switches abruptly when the sign of the projection of the magnetic moment in one of the nonequivalent positions changes, in the present case the spatial orientation of the magnetic moments of the rare-earth sublattices varies continuously. The observed magnetization anomalies, however, are associated with the change in their direction of motion. From the microscopic standpoint, however, the mechanism of these phenomena is the same: the magnetic structure becomes unstable near the points of degeneracy of the states of the f-ions—the magnetic analog of the Jahn–Teller effect.[6,29] The phase transitions at such points is accompanied by inversion of the ground state of the rare-earth ion as a result of crossing of the ground and first excited energy levels of this ion. Note that this interpretation of the anomalies of the magnetization of TYIG for $H < H_{exc}$ was

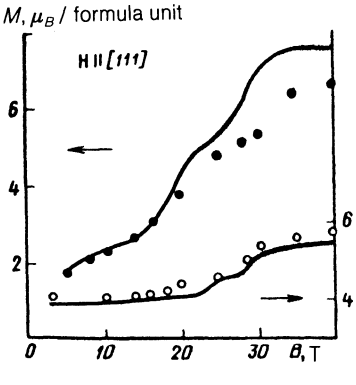

FIG. 3. Computed (dots) and experimental (solid lines) field dependences of the magnetic moment of a $Tb_xY_{3-x}Fe_5O_{12}$ single crystal at $T = 4.2$ K in a magnetic field $B \| [111]$: $x = 0.41$ (dark circles) and 0.1 (light-colored circles).

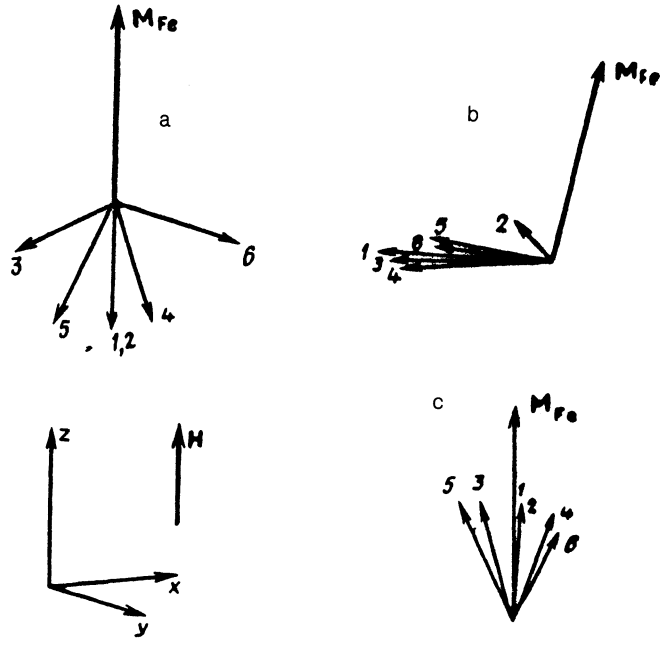

FIG. 5. Evolution of the magnetic structure of a $Tb_{0.1}Y_{2.9}Fe_5O_{12}$ single crystal at $T = 4.2$ K as a function of the external field: a—3 T, b—28 T, c—40 T; $B_{\|}$ [100]. The numbers refer to the rare-earth sublattices.

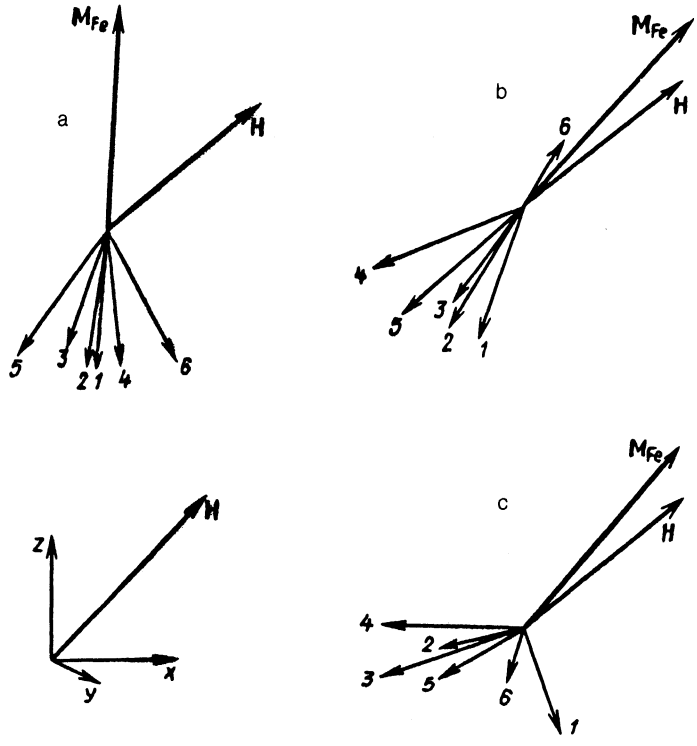

FIG. 6. Evolution of the magnetic structure of a $Tb_{0.26}Y_{2.74}Fe_5O_{12}$ single crystal at $T = 4.2$ K as a function of the external field: a—3 T, b—8 T, c—30 T; $B \| [110]$. The numbers refer to the rare-earth sublattices.

first proposed by Valiev *et al.* in Ref. 27, and their results stimulated significantly the further experimental and theoretical investigations of TYIG, including the present work.

According to the works mentioned, the qualitative phenomenological picture of this phenomenon is as follows. Consider an isolated rare-earth ion in a ferromagnetic matrix. In the initial state (symmetric), characterized by some orientation of the magnetization **M** of the matrix ($\theta = 0$ is the angle of deviation from the initial direction), the ground state of the rare-earth ion is doubly degenerate. The deviation of **M** from the equilibrium position (deformation of the magnetic structure) will immediately result in removal of the degeneracy, i.e., splitting of the levels by ΔE, and the deviation will be linear in θ for small angles:

$$\Delta E_1 = \pm a\theta, \tag{15}$$

where a is the exchange interaction constant between the rare-earth ion and the matrix. Obviously, the ground state energy of the rare-earth ion decreases.

On the other hand, the deviation of **M** increases the energy of the matrix itself at the same time by the amount

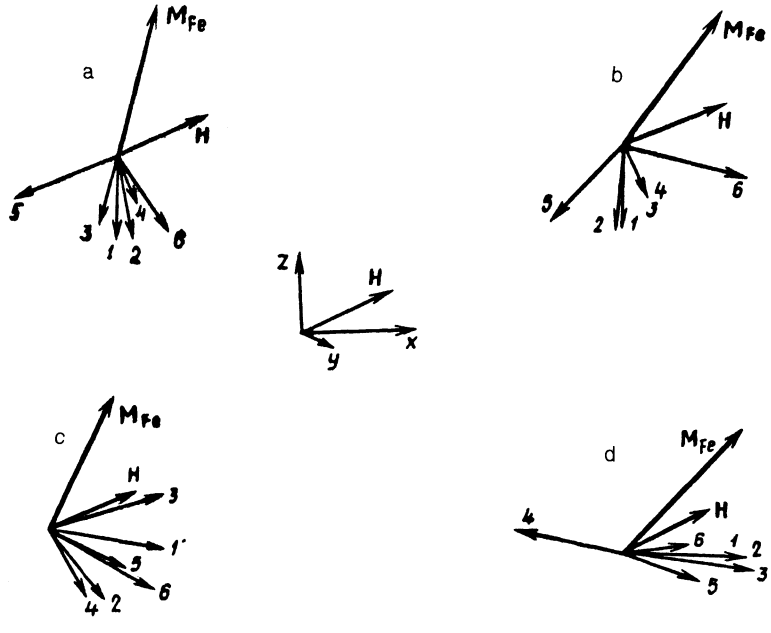

FIG. 7. Evolution of the magnetic structure of a $Tb_{0.41}Y_{2.59}Fe_5O_{12}$ single crystal at $T = 4.2$ K as a function of the external field: a—3 T, b—14 T, c—28 T, d—40 t; $B \| [111]$. The numbers refer to the rare-earth sublattices.

$$\Delta E_2 = {}^1/_2 b\theta^2, \tag{16}$$

where b is the "rigidity" of the magnetic matrix, which in this case is the anisotropy energy and the Zeeman energy of the matrix with an external field. The magnetic structure is determined from the conditions that the energy

$$E = {}^1/_2 b\theta^2 - a|\theta|, \tag{17}$$

be minimum, which occurs at $\theta = \pm a/b$. When the concentrations of ions with degenerate levels are high, a cooperative phase transition occurs. The threshold concentration N_c of the transition, estimated in Ref. 6 using a percolation model, is very small ($N_c \approx 10^{18}$ cm^3), which is almost always met in experiments.

In both cases the states of the system are degenerate because the exchange splitting of the levels due to the external field, which for low concentrations of rare-earth ions is oriented antiparallel to H_{exc}, decreases.[15] The difference between the holmium–yttrium and terbium–yttrium systems is that for the holmium ion the ground state and the excited states close to it are almost "pure" quasidoublets with angular momenta $\pm J$, while the wave functions of the terbium ion are characterized by strong mixing of the basis functions $\Psi(JM)$.[22] As a result of this, magnetization switching of the terbium subsystem in REIG does not occur abruptly, but rather by continuous rotation of the magnetic moments (see Figs. 5–7).

The theoretical calculation of the behavior of the three lowest levels of the terbium ion in TYIG for different concentrations and with different field orientations in all six rare-earth sublattices is illustrated in Figs. 8–10. It is the

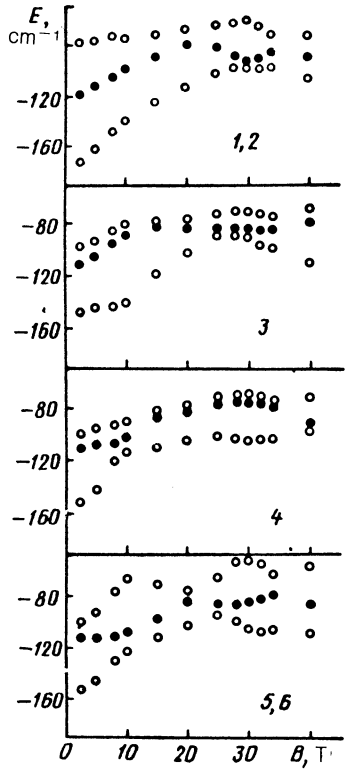

FIG. 9. Energies of the three lowest levels of the Tb^{3+} ion as a function of the magnetic field in a $Tb_{0.26}Y_{2.749}Fe_5O_{12}$ single crystal at $T = 4.2$ K in a magnetic field $B \| [110]$ for all rare-earth sublattices. The numbers 1–6 refer to the sublattices.

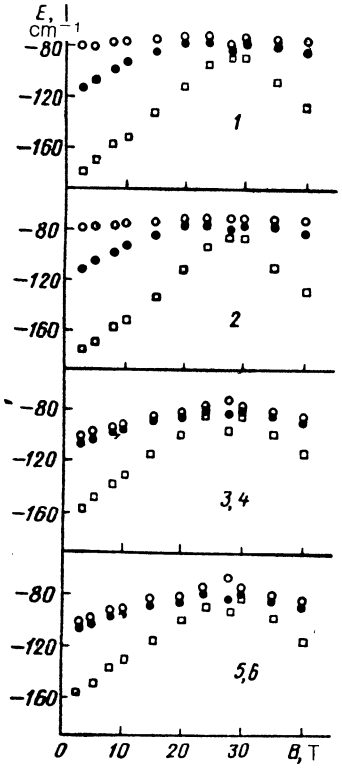

FIG. 8. Energies of the three lowest levels of the Tb^{3+}-ion as a function of the magnetic field in a $Tb_{0.1}Y_{2.9}Fe_5O_{12}$ single crystal at $T = 4.2$ K in a magnetic field $B \| [100]$ for all rare-earth sublattices. The numbers 1–6 refer to the sublattices.

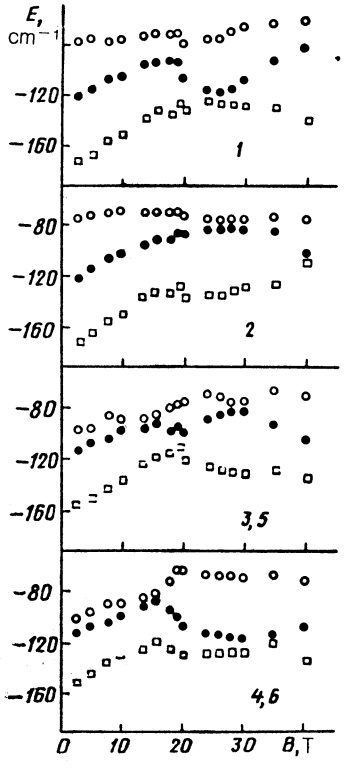

FIG. 10. Energies of the three lowest levels of the Tb^{3+} ion as a function of the magnetic field in a $Tb_{0.41}Y_{2.59}Fe_5O_{12}$ single crystal at $T = 4.2$ K in a magnetic field $B \| [111]$ for all rare-earth sublattices. The numbers 1–6 refer to the sublattices.

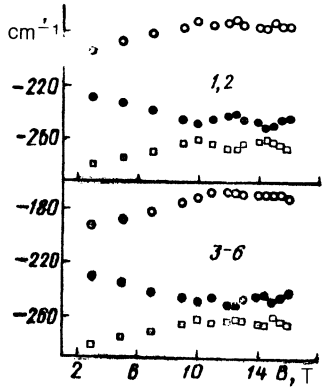

FIG. 11. Energies of the three lowest levels of the Ho^{3+} ion as a function of the magnetic field in a $Ho_{0.2}Y_{2.8}Fe_5O_{12}$ single crystal at $T = 4.2$ K in a magnetic field $B \| [111]$ for all rare-earth sublattices. The numbers 1–6 refer to the sublattices.

behavior of these levels in a magnetic field that is most important to take into account, since the population of the upper-lying levels at $T = 4.2$ K is very small and they do not significantly affect the properties of the Tb^{3+} ion. The field dependence of the energy levels completely confirm the above-state hypothesis that the magnetic analog of the Jahn–Teller effect occurs in TYIG,[27] and not only in fields far from H_{exc} (Ref. 27) but also in the entire range of fields right up to 50 T. The existence of several discontinuities of the moment for a sample with fixed concentration and fixed orientation of the external field is explained by the fact that H_{eff} takes on different values at inequivalent c positions: As the field increases, degeneracy occurs successively in the nonequivalent positions of the rare-earth ions.

The difference between the $Tb_xY_{3-x}Fe_5O_{12}$ and $Ho_xY_{3-x}Fe_5O_{12}$ systems can be seen clearly by comparing Figs. 8–10 with Fig. 11, which displays the computed field dependence of the energy of the three lowest levels of the holmium ion; this dependence was also obtained by the method described above. Near the points of degeneracy the ground state of the Ho^{3+} ion can be considered at low temperatures to be an isolated quasidoublet, whereas this approximation is inadmissible for the Tb^{3+} ion. This is why the Ising model of ordering describes well the magnetic properties of holmium–yttrium iron garnets[28] and is inadequate for the terbium–yttrium system.

In conclusion we make several general remarks about the model presented in this paper. At first glance the number of adjustable parameters B_k^q is quite large because of the low symmetry of the environment of the rare-earth ion. In reality, however, this number is not at all large, if the succession of up to six magnetic phases arising with increasing field due to changes in the ground states of the terbium ions can be explained systematically with the help of all nine parameters. Undoubtedly, it would be desirable to compare the data presented in Table I with the results of other investigations—Raman scattering or optical. This is very difficult to do, since there is no information about B_k^q for $Tb_{0.4}Fe_{2.6}O_{12}$ and the published information on the crystal-field parameters in isomorphous paramagnetic gallates or aluminates[26,30] cannot be used because their lattices differ significantly from the lattice of TYIG due to the presence of significant magnetostriction in the latter case. The only possibility is to extrapolate the results for $Tb_3Fe_5O_{12}$ (Refs. 31 and 32) to low terbium concentrations and low temperatures. This procedure, used for the $B_k^q(x, T)$ dependence employed in the present work,[14] showed that our results on the signs and order of magnitude of the crystal-field parameters (with the exception only of B_6^0 and B_6^2) agree with the data of Ref. 32.

We are sincerely grateful to R. Z. Levitin and A. I. Popov for fruitful discussions and valuable suggestions.

[1]K. P. Belov, *Rare-Earth Magnetics and Their Applications* [in Russian], Nauka, Moscow, 1980.
[2]K. P. Belov, A. K. Zvezdin, A. M. Kadomtseva, and R. Z. Levitin, *Orientational Transitions in Rare-Earth Magnetics* [in Russian], Nauka, Moscow, 1979.
[3]A. G. Gurevich, *Magnetic Resonance in Ferrites and Antiferromagnetics* [in Russian], Nauka, Moscow, 1973.
[4]K. P. Belov, *Magnetothermal Phenomena in Rare-Earth Magnetics* [in Russian], Nauka, Moscow, 1990.
[5]S. V. Vonsovskii, *Magnetism* [in Russian], Nauka, Moscow, 1971.
[6]A. K. Zvezdin, V. M. Matveev, A. A. Mukhin, and A. I. Popov, *Rare-Earth Ions in Magnetically Ordered Crystals* [in Russian], Nauka, Moscow, 1985.
[7]R. F. Druzhinina and V. V. Shkarubskii, Fiz. Tverd. Tela **30**, 595 (1988) [Sov. Phys. Solid State **30**, 342 (1988)].
[8]V. V. Druzhinin, V. V. Shkarubskii, and N. M. Chulkov, Fiz. Tverd. Tela **25**, 2942 (1983) [Sov. Phys. Solid State **25**, 1696 (1983)].
[9]V. V. Shkarubskii, R. F. Druzhinina, and A. S. Lagutin, Fiz. Tverd. Tela **27**, 2059 (1985) [Sov. Phys. Solid State **27**, 1234 (1985)].
[10]M. Gilleo and S. Geller, Phys. Rev. **110**, 73 (1958).
[11]S. Geller and M. Gilleo, Acta Cryst. **10**, 239 (1957).
[12]S. Krupichka, *Physics of Ferrites and Related Oxides* [Russian translation], Mir, Moscow, 1976.
[13]A. Abragam and B. Bleaney, *Electronic Paramagnetic Resonance of Transition Ions*, Clarendon Press, Oxford, 1970.
[14]R. F. Druzhinina, *Candidate's Dissertation in Physical-Mathematical Sciences*, Institute of Atomic Energy, Moscow, 1990.
[15]K. P. Belov, *Ferrites in Strong Magnetic Fields* [in Russian], Nauka, Moscow, 1972.
[16]T. Goto, K. Nakao, and N. Miura, Physica B **155**, 285 (1989).
[17]A. I. Pavlovskii, V. V. Druzhinin, O. M. Tatsenko *et al.* in *Ultrastrong Magnetic Fields* (in Russian], edited by V. M. Titov and G. A. Shvetsov, Nauka, Moscow, 1984, p. 130.
[18]M. E. Foglio and J. H. van Vleck, Proc. Roy. Soc. A **336**, 115 (1974).
[19]A. K. Zvezdin, R. Z. Levitin, A. S. Markosyan *et al.*, Fiz. Tverd. Tela **18**, 387 (1976) [Sov. Phys. Solid State **18**, 225 (1976)].
[20]Y. Yamaguchi and T. Sakuraba, J. Phys. Chem. Solids **41**, 327 (1980).
[21]A. S. Lagutin and A. V. Dmitriev, Fiz. Tverd. Tela **30**, 2959 (1988) [Sov. Phys. Solid State **30**, 1705 (1988)].
[22]R. F. Druzhinina and A. S. Lagutin, Fiz. Tverd. Tela **31**, 304 (1989) [Sov. Phys. Solid State **31**, 1091 (1989)].
[23]N. S. Bakhvalov, *Numerical Methods* [in Russian], Nauka, Moscow, 1975.
[24]H. Jeffreys and B. Swirles, *Methods of Mathematical Physics*, Cambridge University Press, N. Y., 1956.
[25]G. Korn and T. Korn, *Mathematical Handbook for Scientists and Engineers*, McGraw-Hill, N.Y.
[26]M. Guillot, A. Marchand, V. Nekvasil, and F. Tcheou, J. Phys. C **18**, 3545 (1985).
[27]U. V. Valiev, G. S. Krinchik, R. Z. Levitin, and K. M. Mukimov, Pis'ma Zh. Eksp. Teor. Fiz. **29**, 239 (1979) [JETP Lett. **29**, 214 (1979)].
[28]V. I. Silant'ev, A. I. Popov, R. Z. Levitin, and A. K. Zvezdin, Zh. Eksp. Teor. Fiz. **78**, 640 (1980) [Sov. Phys. JETP **51**(2), 323 (1980)].
[29]A. K. Zvezdin, A. I. Popov, and A. A. Mukhin, Zh. Eksp. Teor. Fiz. **72**, 1097 (1977) [Sov. Phys. JETP **45**(3), 573 (1977)].
[30]D. Boal, P. Grunberg, and J. A. Koningstein, Phys. Rev. B **7**, 4757 (1973).
[31]V. Nekvasil, Phys. Status Solidi B **87**, 317 (1978).
[32]Nguyen Hy Hau, P. Porcher, Tran Khanh Vien, and B. Pajot, J. Phys. Chem. Solids **47**, 83 (1986).

Translated by M. E. Alferieff